Journal of Alloys and Compounds 934 (2023) 167992

Contents lists available at ScienceDirect

Journal of Alloys and Compounds

journal homepage: www.elsevier.com/locate/jalcom

High pressure solidification of alloying substitution and promotion of hydrogen storage properties in AB_2-type Y-Zr-Ti-Fe based alloys

Wei Jiang [a,b], Yi Peng [c], Yuchen Mao [a], Hui Wang [a], Liuzhang Ouyang [a], Runze Yu [d], Changqing Jin [c], Min Zhu [a,*]

[a] Guangdong Provincial Key Laboratory of Advanced Energy Storage Materials, School of Materials Science and Engineering, South China University of Technology, Guangzhou 510641, China
[b] Guangzhou Customs Technology Center, Guangzhou 510623, China
[c] Beijing National Laboratory for Condensed Matter Physics, Institute of Physics Chinese Academy of Sciences, Beijing 100190, China
[d] Center for High-Pressure Science and Technology Advanced Research, Beijing 100094, China

ARTICLE INFO

Article history:
Received 5 September 2022
Received in revised form 8 November 2022
Accepted 9 November 2022
Available online 11 November 2022

Keywords:
Hydrogen storage alloys
Laves phase alloys
High pressure solidification

ABSTRACT

Metastable phase has great potential in searching hydrogen storage alloys. In this work, high pressure solidification has been successfully used to realize the supersaturation of Ti in YFe_2 based C15 Laves phase to obtain a metastable $Y_{0.7}Zr_{0.24}Ti_{0.06}Fe_2$ alloy. The segregation of Ti, Y, Zr and related multi-phase formation were substantially suppressed and the obtained HPS alloy contained a primary C15 phase(C15–1) and a secondary C15 phase(C15–2) with 77.1% and 22.9% of the total content, respectively. Meanwhile, the hydrogen absorption and desorption capacities increased substantially. This study proves that the combination of high-pressure solidification and alloying is a very effective method for exploring new hydrogen storage materials with metastable structure and high performance.

1. Introduction

Large scale hydrogen (H) energy storage is a very promising solution for the fluctuated distribution of renewable energy in space and time, and high volumetric density, long life, cheap and safe H storage are essential for that [1,2]. Hydrogen storage alloys (HSAs) offer potential candidates to meet those criteria. However, HSAs, such as $RENi_5$ (RE=rare earth), $TiCr_2$ and TiFe, can only work at ambient temperature and usually in high cost as they contain high proportion of Ni, Ti, Pr, Nd and etc. While Mg based alloys suffer from too high working temperature of about 300 ℃. Thus, these shortcomings hinder large-scale application [3–7]. Therefore, exploration of HSAs that can satisfy the above requirement is still a challenge and of great significance.

It has long been known that the REM_2 Laves phases (M= transition metals) absorb quite high capacity hydrogen at ambient temperature and pressure [8–13]. In particular, YFe_2, which is simply composed of abundant and cheap Fe and Y, can absorb up to 5 H per formula unit (/f.u.) [14–16]. However, REM_2 alloys are irreversible for hydrogen storage due to the unavoidable hydrogen-induced amorphization (HIA) in the de-/hydrogenation process [17–20]. Recently, it has been found that HIA of YFe_2 can be suppressed by simply adding Al, and a REM_2-type reversible HSAs constituted of abundant and cheap resources is developed. Unfortunately, YFe_2-based HSAs exhibit rather low dehydriding equilibrium pressure, leading to incomplete dehydrogenation.

Alloying is an effective method to adjust the properties of HSAs, and the general rule is hydrogen absorption/desorption pressure plateau can increase with the decreasing of lattice constant and increasing of elastic modulus [21–23]. Thus, partial substituting Y with Zr, Ti, Mn, V, Sc, Cr has been applied for YFe_2 and $ZrFe_2$ based alloys [24–28]. Indeed, the dehydriding equilibrium pressure is successfully elevated by Zr addition as the atomic radius of Zr (1.59 Å) is smaller than that of Y atom (1.78 Å). However, it is still partially below atmosphere pressure(0.1013 MPa) [24,25]. It is noted that the atomic radius of Ti (1.45 Å) is much smaller than Y and Zr, and the bulk modulus of Ti (110 GPa) is higher than that of the Y (41 GPa) and Zr (91 GPa). Therefore, it is expected that Ti substitution can further increase the pressure plateau. However, there are still little reports in literatures [25] because only trace amount of Ti can substitute the Zr in $Y(Zr)Fe_2$ phase although Ti has a high mutual solubility with Zr. The addition of more Ti resulted in the inhomogeneity distribution of Y and the formation of Ti-rich phases [25]. Some other elements,

* Corresponding author
E-mail address: memzhu@scut.edu.cn (M. Zhu).

https://doi.org/10.1016/j.jallcom.2022.167992
0925-8388/

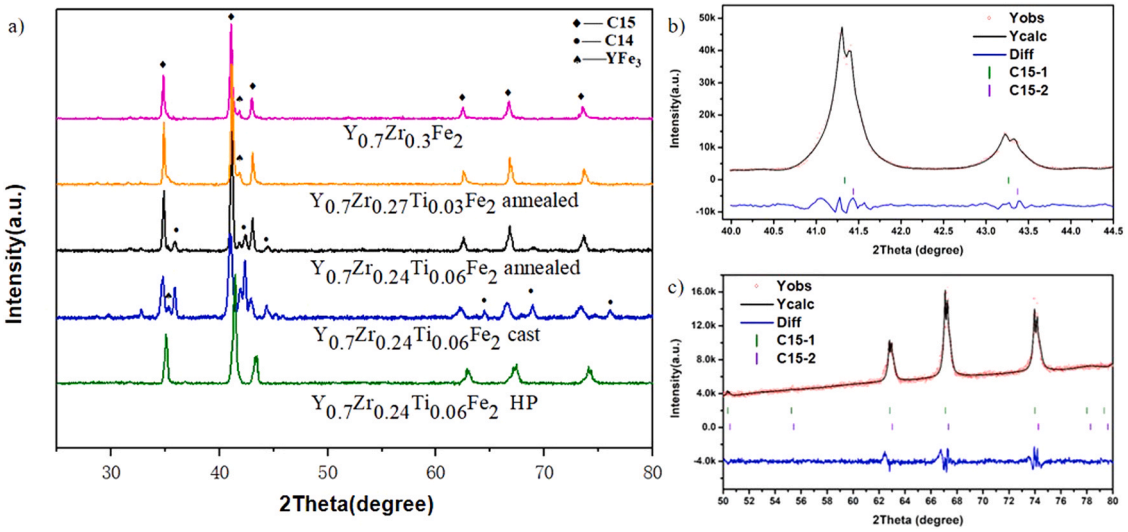

Fig. 1. (a)XRD patterns and (b-c)Rietveld refinement of XRD profiles of $Y_{0.7}Zr_{(0.3-x)}Ti_xFe_2$ alloys prepared by casting and HPS.

such as Sc, are effective, but are not available owing to their very high cost and even toxicity [26].

There is huge difference in microstructure and properties between the metal solidified under high pressure and atmospheric pressure[27]. High pressure has been found to be a powerful tool for controlling the element distribution and phase composition [28]. High pressure solidification (HPS) can effectively increase the solid solubility of solute in alloys and form supersaturated solid solution [29]. The ever increasing chamber dimension and maximum allowable pressure in the high-pressure manufacturing equipment make high-pressure manufacturing became an appealing solution for preparing materials with superb properties nowadays. Matsushita et al. [30]investigated the Mg85Y9Zn6 alloy and found high pressure can transform the 18R-type LPSO to a fine dual-phase structure composed of $D0_3$ and hcp structure. Wang[31] reported in detail the effects of pressure on the structural, mechanical, electronic and vibrational properties of Ethylenediamine bisborane(a hydrogen storage material). To the best knowledge of author, the current studies on hydrogen storage have been mainly focused on materials treated under normal pressure. With the high pressure method is being more widely used in the preparation of metallic materials, studying the effect of high pressure on hydrogen storage materials becomes significant. The present work shows that higher amount of Ti dissolves in YFe_2 based alloy by HPS, and a single C15 phase $Y_{0.7}Zr_{0.2}4Ti_{0.06}Fe_2$ alloy was obtained under high pressure, which could not be realized by conventional melting methods. Element segregation and the formation of harmful phases were inhibited. With the formation of this metastable phase, the hydrogen absorption capacity, desorption capacity and desorption pressure of the alloy increased significantly.

2. Experimental procedure

The $Y_{0.7}Zr_{0.24}Ti_{0.06}Fe_2$, $Y_{0.7}Zr_{0.3}Fe_2$, $Y_{0.7}Zr_{0.27}Ti_{0.03}Fe_2$(reference samples) alloys were prepared by arc-melting under the protection of high purity argon atmosphere (99.999%) in a water-cooled copper crucible with high purity Y, Zr, Fe (purity 99.9%) and Ti (purity 99.99%) metal ingots as raw materials. Before melting, the metal bulks were polished by a grinder to remove the oxidation layer. The samples for high-pressure solidification were cut into cylinders 6 mm in diameter and 6 mm in length. The high-pressure experiments were carried out using a six-anvil apparatus. High pressure was generated by squeezing a cubic pressure medium containing a sample with six anvils made of tungsten carbide. An internal heater located in the cubic pressure medium generates the high temperature. Typically, the heater was composed of graphite and was in contact with the top and bottom electrodes in the cubic pressure medium, supplying electric current through anvils. When an electric current was supplied to the heater, the sample was heated by Joule heat. The pressure was applied before increasing the temperature. Sample was heated for 1 h at relatively stable temperature(~1500 K) and pressure(5.5 GPa), then stopped heating and the anvils were cooled by chilled water to room temperature. After the sample was cooled down, the applied pressure was released. The microstructure was characterized by X-ray diffraction (XRD, Empyrean diffractometer, Cu-Ka radiation λ = 1.5406 Å) and scanning electron microscope (SEM) equipped with energy dispersive X-ray spectroscopy (EDS). The hydrogen storage properties were measured by using a Sievert-type automatic gas reaction controller (Advanced Materials Corporation) with reservoir in 63.546 ml. Before measurement, the samples about 1 g were activated under dynamic vacuuming condition below 0.01 bar at 473 K for 2 h. The isothermal hydrogenation kinetics was measured under 4 MPa H_2 at 373 K, while the desorption PCI curve was examined at 473 K.

3. Results and discussion

Fig. 1 shows the XRD patterns of $Y_{0.7}Zr_{(0.3-x)}Ti_xFe_2$ (x = 0.03,0.06) alloys prepared by different process, and the reference melted ternary $Y_{0.7}Zr_{0.3}Fe_2$ alloy. It can be seen that all the melted quaternary alloys consist of predominant Y(Zr)Fe_2 Laves phase of C15 structure. In addition to the C15 phase, there are some weak peaks which corresponded to C14 Laves phase and YFe_3 phase. Especially, the YFe_3 phase is present in all the melting alloys, even though the alloys are treated by a long time of high-temperature annealing, which is consistent with Y-Fe-Al and Y-Zr-Fe alloys [24]. This is because the Gibbs free energy of YFe_3 and YFe_2 is very close [32], the YFe_3 phase is easily formed in the vicinity of YFe_2 where the local Y content is low if the alloys composition fluctuated. Moreover, there are a large amount of C14 phase in the cast and annealed $Y_{0.7}Zr_{0.24}Ti_{0.06}Fe_2$ alloys, which demonstrates the addition of Ti could not substitute Y and Zr but results in C14 phase formation under conventional preparation condition. In contrast, the alloy prepared by HPS contains only C15 phase without the presence of C14 phase and YFe_3 phase. This demonstrates that high pressure effectively changing the phase equilibrium of the alloy and forces the dissolving of Ti into C15 phase to form a metastable phase. Consequently, the alloy should also become more homogeneous. However, it should be

Table 1
The phase contents and structure parameters.

Phase		C15-1	C15-2
Phase contents		77.10	22.90
Space group		Fd-3mS	Fd-3mS
Structure parameters	a (Å)	7.2391(9)	7.2206(5)
	b(Å)	7.2391(9)	7.2206(5)
	c(Å)	7.2391(9)	7.2206(5)
	α(°)	90	90
	β(°)	90	90
	γ(°)	90	90

noted that the diffraction peaks of HPS sample are a little asymmetric, which indicates the presence of a small amount of another C15 phase with the lattice constant close to the main C15 phase. Therefore, Rietveld analysis was carried out to fitting the diffract gram, as it is shown in Fig. 1, and two C15 phases, including primary phase (named as C15–1 here) and secondary phase (named as C15–2), are identified with proportion being 77.1% and 22.9%, respectively. The lattice constants of C15–1 and C15–2 are very close, being 7.2391(9) Å and 7.2206(5) Å, respectively. The phase contents and structure parameters are displayed in Table 1.

The microstructure of those $Y_{0.7}Zr_{0.24}Ti_{0.06}Fe_2$ quaternary alloys was further investigated by SEM equipped with EDS. There is obvious element segregation in the as-cast $Y_{0.7}Zr_{0.24}Ti_{0.06}Fe_2$ alloy, especially the Ti, as shown in Fig. 2(a). The segregation region of Ti corresponds to the C14 phase. In contrast, after HPS, element segregation is suppressed, especially Ti element distribution is uniform, as shown in Fig. 2(b). With respect to the Zr and Y, comparing Fig. 2(a) with Fig. 2(b), there are segregation region of Zr and depletion region of Y in both melting sample and HPS sample, and those two regions are coincident, which means that Y and Zr are repulsive in the alloy in the presence of Ti. Nevertheless, the segregation of Zr and Y is much less obvious in the HPS alloys. In accordance to the XRD results, the Zr segregation (Y depletion) region should corresponds to C15–2 phase. According to the EDS analysis, the average composition of C15–1 and C15–2 phase is $Y_{22.74}Zr_{5.81}Ti_{1.31}Fe_{70.14}$ and $Y_{11.92}Zr_{14.94}Ti_{3.87}Fe_{69.27}$, respectively. Thus, it is understood that the microstructure of the alloy is entirely changed by HPS. Firstly, Ti dissolves into the YFe_2 based C15 phase, which could not be achieved in conventional preparation; Secondly, the alloy contains two C15 phase with complementary Zr and Y content, while the C14 phase presented in melting alloy disappears entirely.

It is known that Y and Ti elements are immiscible below 1273 K [33]. As a result, the addition of Ti seriously affects the homogeneity of Y in the Y-Zr-Ti-Fe alloy, and also leads to the formation of Ti rich phase. As well known, HPS changes the melting point, growth rate, undercooling degree and solute diffusion coefficient of the alloy. Increasing the pressure will increase the viscosity of the liquid metal, so that it can be assumed that there is no convection in the melt. Moreover, as the pressure increasing, the solute diffusivity decreases exponentially. When the solidification pressure is over 3 GPa, the solute diffusion coefficient ratio of high pressure to atmospheric pressure is 10^{-9}, which is very easy to cause solute trapping. Thus, the HPS suppresses element segregation and forms supersaturated C15 phase.

Substantial influence is achieved on hydrogen storage properties by the HPS formed unique microstructure. Fig. 3(a) and 3(b) shows the hydrogen absorption kinetic curves under 4 MPa H_2 pressure at 373 K and dehydrogenation PCI curves at 473 K. It is illustrated that the absorption capacity is only 1.17 wt% for the as-cast $Y_{0.7}Zr_{0.24}Ti_{0.06}Fe_2$ alloy, and is even lower than that of the $Y_{0.7}Zr_{0.3}Fe_2$ ternary alloy (1.60 wt%) [24]. It is obvious that the added Ti does not play positive role because it can not dissolve into C15 phase but results in the formation of large quantities of Zr-Ti-Fe C14 secondary phase, and thus, the amount of hydrogen absorption phase(C15) decreases significantly. After HPS treatment, the hydrogen absorption capacity of the alloy increases to 2.06 wt%, which is much higher than that of the as-cast alloy and the $Y_{0.7}Zr_{0.3}Fe_2$ ternary alloy both. The hydrogen desorption pressure is also greatly elevated for the HPS treated samples, which leads to greatly increase dehydrogenation capacity, being 0.69 wt% at 0,01 MPa. This demonstrates that Ti addition can greatly promote the reversible hydrogen storage of YFe_2 based Laves phase alloys if Ti can substantially dissolve into its primary C15 Laves phase. As mentioned before, the equilibrium dehydrogenation pressure of the hydrogen storage alloy is proportional to the ratio of the bulk modulus B to the crystal cell volume V, i.e. $\ln P \propto B/V$. The addition of Ti increases the bulk modulus and elastic limit of the alloy (Ti:113 GPa, Y:41 GPa, Zr:91 GPa, Fe:168 GPa). In addition, the lattice constants of the C15 phases also decreases by Ti substitution. The lattice constant of C15 phase in $Y_{0.7}Zr_{0.3}Fe_2$ and as-cast $Y_{0.7}Zr_{0.27}Ti_{0.06}Fe_2$ alloy are 7.279 Å and 7.2732 Å respectively, while they are 7.2391 Å and 7.2206 Å, respectively, for C15–1 and C15–2 in $Y_{0.7}Zr_{0.27}Ti_{0.06}Fe_2$ alloy treated HPS. This demonstrates the significant cell volume decrease of C15 phase with the dissolving of Ti, being 1.633% and 2.385% for C15–1 and C15–2 comparing with the original C15 phase, respectively. Therefore, the dehydrogenation plateau pressure of the alloy increases and the dehydrogenation performance is improved.

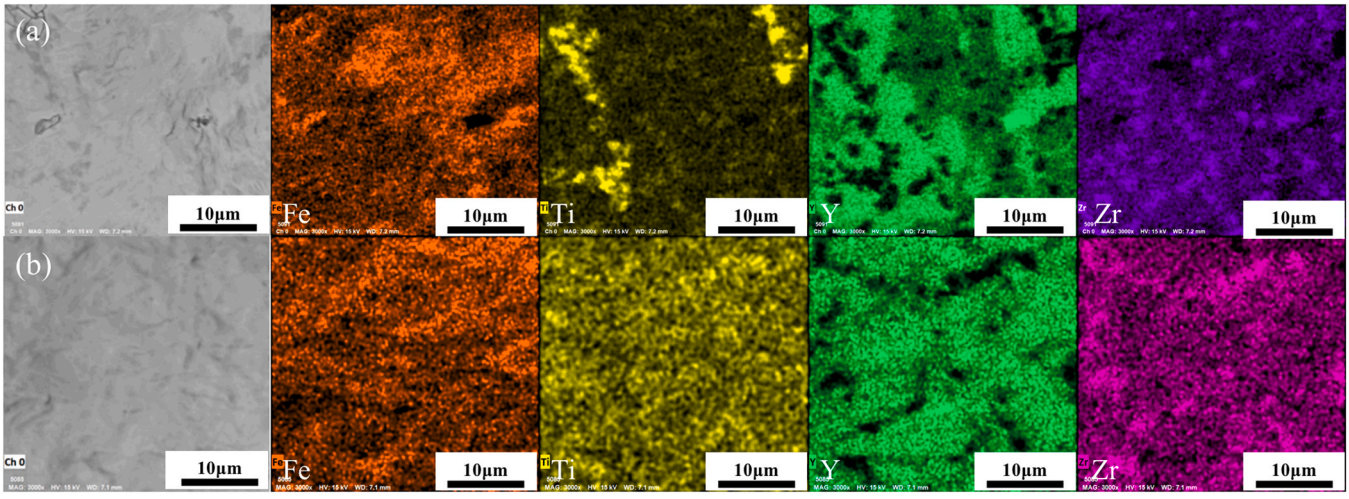

Fig. 2. The microstructure and element distribution in (a) the as-cast and (b) HPS processed $Y_{0.7}Zr_{0.24}Ti_{0.06}Fe_2$ alloy.

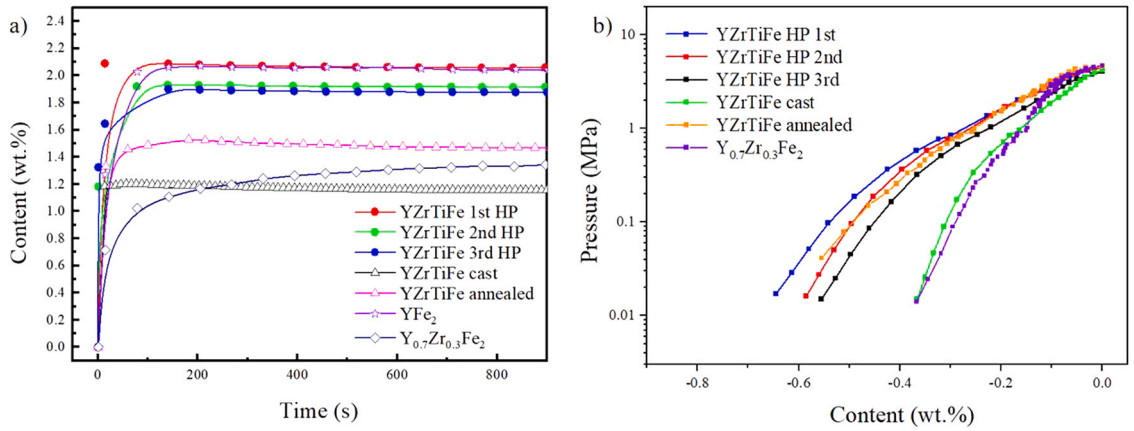

Fig. 3. (a)Hydrogen absorption kinetic curves under 4 MPa H_2 at 373 K and (b)Dehydrogenation PCI curves at 473 K for the as-cast and HPS processed $Y_{0.7}Zr_{0.24}Ti_{0.06}Fe_2$ alloys.

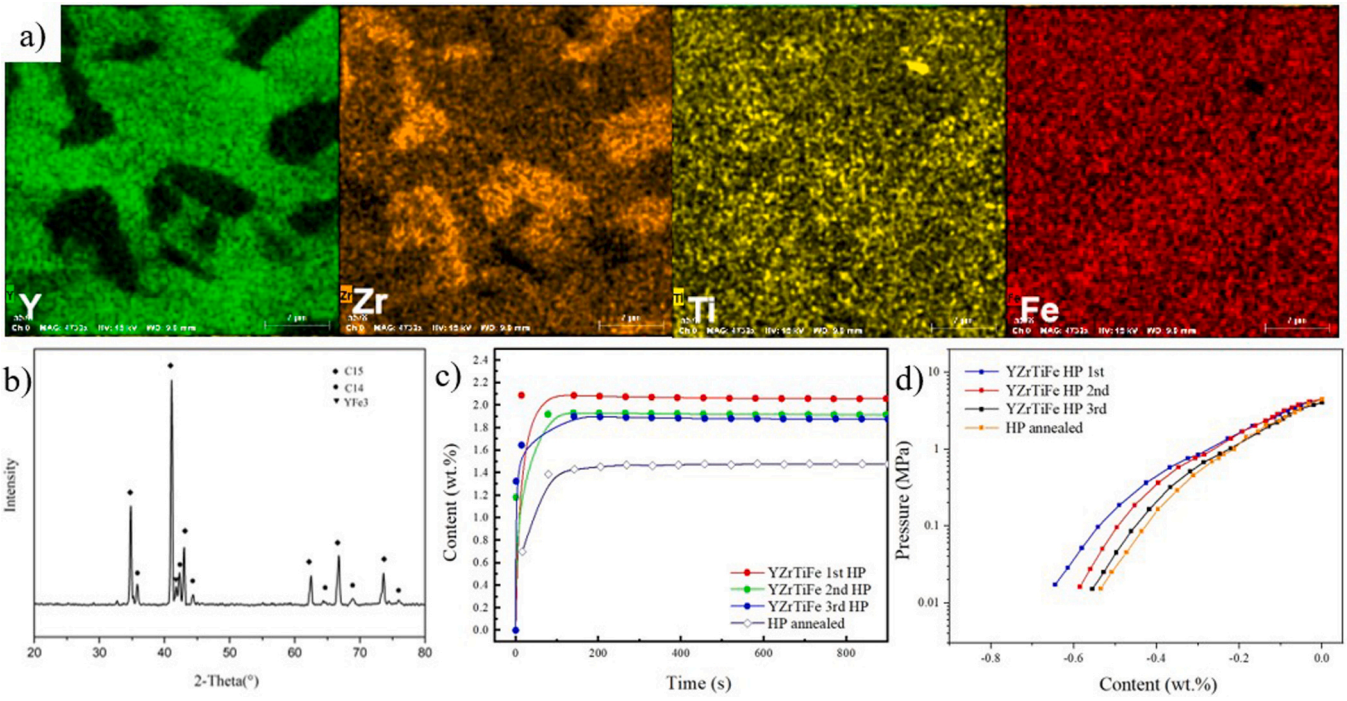

Fig. 4. The microstructure and properties of the annealed HPS Y0.7Zr0.24Ti0.06Fe2 alloy: (a) The microstructure and elements distribution; (b) XRD pattern; (c) Hydrogen absorption kinetic curves under 4 MPa H2 at 373 K; (d)Dehydrogenation PCI curves at 473 K.

Although the new C15 phase obtained by HPS is supersaturated in Ti and metastable, it is significant that the HPS C15 alloy is quite stable under hydrogenation/dehydrogenation cycling. As it is shown in Fig. 3, the hydrogen absorption capacity remains at 1.91 wt% and 1.87 wt%, and the dehydrogenation capacity remains at 0.62% and 0.59%, in the following two cycles. To further examine the stability of the HPS C15 phase, the HPS samples were annealed in sealed quartz ampoules at 573 K for 48 h. The heat treatment temperature was determined by DSC analysis which demonstrates that no thermal reaction existed below 573 K. After heat treatment, the segregation of Y and Zr becomes much more obvious, as shown in Fig. 4(a), but there is still no obvious segregation of Ti element. The XRD analysis, as shown in Fig. 4(b), reveals that the metastable C15 phase is decomposed and the obtained microstructure contains C15 phase, C14 phase and YFe_3 phase. The lattice constant of C15 phase changes from 7.239 of HPS alloy to 7.269 of annealed alloy with the composition of $Y_{24.5}Zr_{5.91}Ti_{1.88}Fe_{67.7}$, and the composition of C14 phase is $Y_{5.17}Zr_{23.76}Ti_{3.3}Fe_{67.76}$. The proportions of the two phases are 85% and 14%. As a result, the hydrogen absorption capacity changes to 1.47% and the dehydrogenation capacity is 0.53%. Although the properties deteriorate a little comparing to that of HPS alloy, it is still much better than the as-cast $Y_{0.7}Zr_{0.24}Ti_{0.06}Fe_2$ alloys. This provides strong indication for design of the YFe_2 based Laves phase alloys.

4. Conclusion

In summary, high pressure solidification (HPS) has been successfully used to realize the supersaturated solid solution of Ti in YFe_2 based C15 Laves phase in $Y_{0.7}Zr_{0.24}Ti_{0.06}Fe_2$ alloy. The segregation of Ti, Y and Zr and related multi-phase formation are substantially suppressed and the HPS alloy contains a primary C15 phase(C15–1) and a secondary C15 phase(C15–2) with proportion of 77.1% and 22.9%, respectively. The C15–1 phase and the C15–2 phase has composition of $Y_{22.74}Zr_{5.81}Ti_{1.31}Fe7_{0.14}$ and $Y_{11.92}Zr_{14.94}Ti_{3.87}Fe_{69.27}$, respectively, and their lattice constants are very close to each other, being 7.23919 Å and 7.22065 Å. The formation of this meta-stable structure promotes greatly the reversible hydrogen storage properties of YFe_2 based Laves phase alloys. The

hydrogen absorption/desorption capacity reaches 2.06 wt% /0.69% (at 0.01 MPa) for HPS alloy, respectively, while it is 1.17 wt% and 0.36 wt% for the cast alloy. The hydrogen storage properties remain quite stable with hydrogen absorption/desorption capacity being 1.91 wt%/0.62 wt% and 1.87 wt%/0.59 wt%, respectively in following two cycles. Heating at higher temperature of 573 K, the HPS formed metastable phases transforms to stable state composed of C15 phase, C14 phase and YFe_3 phase, and the major hydrogen storage properties still remains, although they deteriorate a little. This study demonstrates that there is still great space to promote the hydrogen storage properties of YFe_2 based alloys and HPS is a very effective method for that.

CRediT authorship contribution statement

Wei Jiang: Conceptualization, Investigation, Writing – original draft, Writing – review & editing. **Yi Peng:** Investigation. **Yuchen Mao:** Investigation. **Hui Wang:** Resources, **Liuzhang Ouyang:** Resources. **Runze Yu:** Resources, Writing – review & editing. **Changqing Jin:** Resources, Writing – review & editing. **Min Zhu:** Supervision, Funding acquisition.

Data Availability

The authors do not have permission to share data.

Declaration of Competing Interest

The authors declare that they have no known competing financial interests or personal relationships that could have appeared to influence the work reported in this paper.

Acknowledgements

This work was supported by the National Natural Science Foundation of China [No. 51621001, 51901080 and 22171283], and Guangdong Basic and Applied Basic Research Foundation [No. 2019A1515010039], Beijing Nature Science Foundation (2202059).

Appendix A. Supporting information

Supplementary data associated with this article can be found in the online version at doi:10.1016/j.jallcom.2022.167992.

References

[1] A.Z. Arsad, M.A. Hannan, A.Q. Al-Shetwi, M. Mansur, K.M. Muttaqi, Z.Y. Dong, F. Blaabjerg, Hydrogen energy storage integrated hybrid renewable energy systems: A review analysis for future research directions, Int. J. Hydrog. Energy 47 (2022) 17285–17312, https://doi.org/10.1016/j.ijhydene.2022.03.208
[2] M.D. Scovell, Explaining hydrogen energy technology acceptance: a critical review, Int. J. Hydrog. Energy 47 (2022) 10441–10459, https://doi.org/10.1016/j.ijhydene.2022.01.099
[3] J. Bellosta von Colbe, J.-R. Ares, J. Barale, M. Baricco, C. Buckley, G. Capurso, N. Gallandat, D.M. Grant, M.N. Guzik, I. Jacob, E.H. Jensen, T. Jensen, J. Jepsen, T. Klassen, M.V. Lototskyy, K. Manickam, A. Montone, J. Puszkiel, S. Sartori, D.A. Sheppard, A. Stuart, G. Walker, C.J. Webb, H. Yang, V. Yartys, A. Züttel, M. Dornheim, Application of hydrides in hydrogen storage and compression: achievements, outlook and perspectives, Int. J. Hydrog. Energy 44 (2019) 7780–7808, https://doi.org/10.1016/j.ijhydene.2019.01.104
[4] [1], J. Yao, Z. Wu, H. Wang, F. Yang, J. Ren, Z. Zhang, Application-oriented hydrolysis reaction system of solid-state hydrogen storage materials for high energy density target: A review, J. Energy Chem. 74 (2022) 218–238, https://doi.org/10.1016/j.jechem.2022.07.009
[5] Y. Sui, Z. Yuan, D. Zhou, T. Zhai, X. Li, D. Feng, Y. Li, Y. Zhang, Recent progress of nanotechnology in enhancing hydrogen storage performance of magnesium-based materials: A review, Int. J. Hydrog. Energy 47 (2022) 30546–30566, https://doi.org/10.1016/j.ijhydene.2022.06.310
[6] Z. Chen, K.O. Kirlikovali, K.B. Idrees, M.C. Wasson, O.K. Farha, Porous materials for hydrogen storage, Chem 8 (2022) 693–716, https://doi.org/10.1016/j.chempr.2022.01.012
[7] J. Zhang, S. Yan, H. Qu, Recent progress in magnesium hydride modified through catalysis and nanoconfinement, Int. J. Hydrog. Energy 43 (2018) 1545–1565, https://doi.org/10.1016/j.ijhydene.2017.11.135
[8] J.B. Ponsoni, V. Aranda, T. da, S. Nascimento, R.B. Strozi, W.J. Botta, G. Zepon, Design of multicomponent alloys with C14 laves phase structure for hydrogen storage assisted by computational thermodynamic, Acta Mater. 240 (2022) 118317, https://doi.org/10.1016/j.actamat.2022.118317
[9] V.A. Yartys, M.V. Lototskyy, Laves type intermetallic compounds as hydrogen storage materials: a review, J. Alloy. Compd. 916 (2022) 165219, https://doi.org/10.1016/j.jallcom.2022.165219
[10] S. Dey, S. Kumari, P.A. Deshpande, A DFT analysis unravelling hydrogen sorption pathways in Laves phase Cu2Cd, Appl. Surf. Sci. 605 (2022) 154721, https://doi.org/10.1016/j.apsusc.2022.154721
[11] Y. Yan, Z. Li, Y. Wu, S. Zhou, Hydrogen absorption-desorption characteristic of (Ti0.85Zr0.15)1.1Cr1-xMoxMn based alloys with C14 Laves phase, Prog. Nat. Sci. Mater. Int. 32 (2022) 143–149, https://doi.org/10.1016/j.pnsc.2022.03.001
[12] W. Liu, E. Bykov, S. Taskaev, M. Bogush, V. Khovaylo, N. Fortunato, A. Aubert, H. Zhang, T. Gottschall, J. Wosnitza, F. Scheibel, K. Skokov, O. Gutfleisch, A study on rare-earth Laves phases for magnetocaloric liquefaction of hydrogen, Appl. Mater. Today 29 (2022) 101624, https://doi.org/10.1016/j.apmt.2022.101624
[13] C. Qin, H. Wang, J. Liu, L. Ouyang, M. Zhu, Tuning hydrogen storage thermodynamic properties of ZrFe2 by partial substitution with rare earth element Y, Int. J. Hydrog. Energy 46 (2021) 18445–18452, https://doi.org/10.1016/j.ijhydene.2021.03.012
[14] S.-R. Yuan, L. Ouyang, M. Zhu, Y.-J. Zhao, Theoretical study of YFe2H (x = 0–5): a comparison between cubic and orthorhombic phases, J. Magn. Magn. Mater. 460 (2018) 61–68, https://doi.org/10.1016/j.jmmm.2018.03.033
[15] E. Téliz, M. Abboud, R. Faccio, M. Esteves, F. Zinola, V. Díaz, Hydrogen storage in AB2 hydride alloys: Diffusion processes analysis, J. Electroanal. Chem. 879 (2020) 114781, https://doi.org/10.1016/j.jelechem.2020.114781
[16] Z. Li, H. Wang, L. Ouyang, J. Liu, M. Zhu, Achieving superior de-/hydrogenation properties of C15 Laves phase Y-Fe-Al alloys by A-side substitution, J. Alloy. Compd. 787 (2019) 158–164, https://doi.org/10.1016/J.JALLCOM.2019.02.074
[17] Z. Li, H. Wang, L. Ouyang, J. Liu, M. Zhu, Increasing de-/hydriding capacity and equilibrium pressure by designing non-stoichiometry in Al-substituted YFe2compounds, J. Alloy. Compd. 704 (2017) 491–498, https://doi.org/10.1016/J.JALLCOM.2017.02.064
[18] N. Ding, D. Liu, W. Liu, J. Zhao, J. Lin, L. Wang, F. Liang, Excellent kinetics and effective hydrogen storage capacity at low temperature of superlattice rare-earth hydrogen storage alloy by solid-phase treatment, J. Phys. Chem. Solids 161 (2022) 110402, https://doi.org/10.1016/j.jpcs.2021.110402
[19] W. Jiang, Y. Chen, M. Hu, C. Zeng, C. Liang, Rare earth-Mg-Ni-based alloys with superlattice structure for electrochemical hydrogen storage, J. Alloy. Compd. 887 (2021) 161381, https://doi.org/10.1016/j.jallcom.2021.161381
[20] K. Suzuki, K. Ishikawa, K. Aoki, J.M. Cadogan, M. Ishimaru, Y. Hirotsu, Exchange interactions in hydrogen-induced amorphous YFe2, J. Non Cryst. Solids 353 (2007) 748–752, https://doi.org/10.1016/j.jnoncrysol.2006.12.069
[21] Z. Lu, J. Wang, Y. Wu, X. Guo, W. Xiao, Predicting hydrogen storage capacity of V-Ti-Cr-Fe alloy via ensemble machine learning, Int. J. Hydrog. Energy 47 (2022) 34583–34593, https://doi.org/10.1016/j.ijhydene.2022.08.050
[22] A. Kumar, T.P. Yadav, N.K. Mukhopadhyay, Notable hydrogen storage in Ti-Zr-V-Cr-Ni high entropy alloy, Int. J. Hydrog. Energy 47 (2022) 22893–22900, https://doi.org/10.1016/j.ijhydene.2022.05.107
[23] [1], Z. Han, Z. Yuan, T. Zhai, D. Feng, H. Sun, Y. Zhang, Effect of yttrium content on microstructure and hydrogen storage properties of TiFe-based alloy, Int. J. Hydrog. Energy (2022), https://doi.org/10.1016/j.ijhydene.2022.09.227
[24] H. Pang, Z. Li, C. Zhou, H. Wang, L. Ouyang, S. Yuan, Y. Zhao, M. Zhu, Achieving the dehydriding reversibility and elevating the equilibrium pressure of YFe2 alloy by partial Y substitution with Zr, Int. J. Hydrog. Energy 43 (2018) 14541–14549, https://doi.org/10.1016/J.IJHYDENE.2018.05.161
[25] Y.Z. Chen, H.L. Pang, H. Wang, J.W. Liu, L.Z. Ouyang, M. Zhu, Exploration of Ti substitution in AB2-type Y Zr Fe based hydrogen storage alloys, Int. J. Hydrog. Energy 44 (2019) 29116–29122, https://doi.org/10.1016/j.ijhydene.2019.04.139
[26] S. Zhao, H. Wang, J. Liu, Exploring the hydrogen-induced amorphization and hydrogen storage reversibility of Y(Sc)0.95Ni2 laves phase compounds, Mater. (Basel) 14 (2021) 276, https://doi.org/10.3390/ma14020276
[27] C. Zhou, H. Wang, L.Z. Ouyang, J.W. Liu, M. Zhu, Achieving high equilibrium pressure and low hysteresis of Zr-Fe based hydrogen storage alloy by Cr/V substitution, J. Alloy. Compd. 806 (2019) 1436–1444, https://doi.org/10.1016/j.jallcom.2019.07.170
[28] Z. Li, H. Wang, L. Ouyang, J. Liu, M. Zhu, Reversible hydriding in YFe2-xAlx (x = 0.3, 0.5, 0.7) intermetallic compounds, J. Alloy. Compd. 689 (2016) 843–848, https://doi.org/10.1016/J.JALLCOM.2016.08.003
[29] W. Jiang, C. Zou, Y. Chen, Z. Wei, The effect of pressure-induced Mg64Zn15Y21 phase on the mechanical properties of Mg-Zn-Y alloy, J. Alloy. Compd. 840 (2020) 155682, https://doi.org/10.1016/j.jallcom.2020.155682
[30] M. Matsushita, T. Nagata, J. Bednarcik, N. Nishiyama, S. Kawano, S. Iikubo, Y. Kubota, R. Morishita, T. Irifune, M. Yamasaki, Key factor for the transformation from hcp to 18r-type long-period stacking ordered structure in Mg alloys, Mater. Trans. 60 (2019) 237e245.
[31] W. Wang, Q. Liu, Z. Liu, High-pressure study of hydrogen storage material ethylenediamine bisborane from first-principle calculations, J. Mater. Res. Technol. 19 (2022) 3474–3483, https://doi.org/10.1016/j.jmrt.2022.06.084
[32] P.R. Subramanian, J.F. Smith, Thermodynamics of formation of Y-Fe alloys, Calphad 8 (1984) 295–305, https://doi.org/10.1016/0364-5916(84)90033-6
[33] W. GONG, T. CHEN, D. LI, Y. LIU, Thermodynamic investigation of Fe-Ti-Y ternary system, Trans. Nonferrous Met. Soc. China 19 (2009) 199–204, https://doi.org/10.1016/S1003-6326(08)60252-6